ELSEVIER

Journal of Membrane Science 132 (1997) 1–21

journal of MEMBRANE SCIENCE

Electro-osmotic pumping of sodium chloride solutions

J.J. Schoeman[a,*], Jacobus F. van Staden[b]

[a]*ENVIRONMENTEK, CSIR, PO Box 395, Pretoria 0001, South Africa*
[b]*Department of Chemistry, University of Pretoria, Pretoria 0002, South Africa*

Received 24 October 1995; received in revised form 21 October 1996; accepted 1 November 1996

Abstract

Electro-osmotic pumping (EOP) theory and its characteristics (transport numbers, brine concentration, current density, current efficiency, electro-osmotic coefficients, etc.) of Selemion AMV and CMV ion-exchange membranes were studied. The brine concentration increased with increase in current density and feed water concentration. Current efficiency was nearly constant in a wide range of current densities and feed water concentrations. The water flow through the membranes also increased with increasing current density and feed water concentration. The increase in water flow increased the current efficiency significantly. Consequently, water flow through electrodialysis (ED) membranes had a positive effect on ED. Electro-osmotic coefficients decreased with increasing feed water concentration. Osmotic flow in EOP–ED decreased relative to the total flow with increasing current density while the electro-osmotic flow increased relative to the osmotic flow. Osmotic flow significantly contributes to the total water flow in EOP. Selemion AMV and CMV membranes performed well for salt concentration. A simple membrane potential measurement has been demonstrated to function reasonably satisfactorily to predict membrane performance for salt concentration.

Keywords: Electro-osmotic pumping; Electrodialysis; Ion-exchange membranes; Membrane potential; Transport numbers; Models; Membrane performance prediction; Current efficiency; Brine concentration; Electro-osmotic coefficients; Osmotic flow; Electro-osmotic flow

1. Introduction

Electro-osmotic pumping (EOP) is a variant of conventional electrodialysis (ED) that should be suitable for concentration/desalination of saline waters [1]. In EOP, brine is not circulated through the brine compartments, but is evolved in a closed cell. Brine enters the cell as electro-osmotic and osmotic water and leaves the cell by electro-osmotic pumping. This leads to very high concentration factors (high brine concentration) which results in high recovery of product water and a small volume of brine gets disposed. The relatively simple design of an EOP–ED stack, the possibility that EOP–ED may be less expensive than conventional ED and the small brine volume produced, are the major advantage of EOP–ED [1].

Electro-osmotic pumping of sodium chloride solutions has been described by Garza [1]; Garza and Kedem [2]; Kedem et al. [3]; Kedem and Cohen [4]; and Kedem and Bar-On [5]. Water and salt fluxes were studied through ion-exchange membranes as a function of current density and feed concentration and

*Corresponding author.

PII S0376-7388(96)00339-0

mathematical models were developed to describe the experimental data [1]. Kedem and Bar-On [5] have reported that current efficiency determined in EOP experiments was close to the value expected from transport number determinations when sodium chloride solutions were electrodialyzed. Kedem and Bar-On [5] have also reported that apparent transport numbers gave a lower estimate of current efficiency in ED. However, only results for sodium chloride solutions at 0.1 mol/l (5.85 g/l) feed concentration and one commercially available ion-exchange membrane, viz. Selemion AMV and CMV, were reported. It would be very useful if membrane performance for concentration/desalination applications could be accurately predicted from transport numbers obtained from simple potential measurements. Information in this regard for ion-exchange membranes that can be used for saline effluent treatment is limited.

Saline effluents frequently occur in industry. These effluents have the potential to be treated with EOP–ED for water and chemical recovery and effluent volume reduction. Little information, however, could be found in the literature regarding EOP characteristics (brine volume, current efficiency, electro-osmotic coefficients, etc.) of membranes suitable for EOP–ED of saline solutions. Consequently, information regarding EOP characteristics of commercially available ion-exchange membranes, suitable for saline solution treatment, is insufficient and information in this regard will be necessary to select membranes suitable for EOP–ED of saline effluents.

The objectives of this study were therefore to: (a) Consider EOP–ED theory; (b) Study firstly the EOP–ED characteristics (transport numbers, brine concentration, current density, current efficiency, electro-osmotic coefficients, etc.) of the well-known Selemion AMV and CMV ion-exchange membranes over a wide concentration range in a single cell pair, and (c) Determine whether membrane performance could be predicted effectively from simple transport number determinations and existing models.

2. Theory of electro-osmotic pumping–the stationary state–brine concentration and volume flow

2.1. Ion fluxes and volume flow

In the unit cell flow regime, ED becomes a three-port system like reverse osmosis. The feed solution is introduced between the concentrating cells, passes between the cells and leaves the system. The permeate composition is completely determined by membrane performance under the conditions of the process. A schematic diagram of a unit cell showing ion and water fluxes in the system is shown in Fig. 1 [1]. For a univalent salt like sodium chloride, the current density

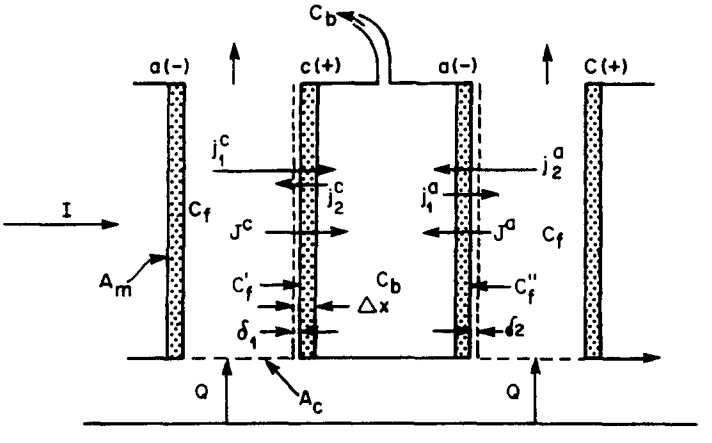

Fig. 1. Representation of fluxes in the ED unit-cell system. c and a indicate the cation- and anion-exchange membranes and subscripts 1 and 2 refer to the cation and anion, respectively (univalent salts); Δx: membrane thickness; δ: effective Nernst layer; c_f: feed concentration; c_b: brine concentration; J^c and J^a: water fluxes; j^a and j^c anion and cation currents. A_m: effective membrane area; A_c: transversal area of the dialysate compartment; and Q: flow of dialysate. The arrows show the direction of the fluxes.

through a cation-exchange membrane is related to the ion fluxes [1]:

$$I = F(z_1 j_1^c + z_2 j_2^c) \quad (1)$$

$$= F(|j_1^c| + |j_2^c|) \quad (2)$$

where z_1=1 cation, z_2=−1 anion and j_1^c and j_2^c are the cation and anion fluxes through the cation-exchange membrane, respectively.

Effective transport numbers are defined as follows [1,2]:

$$\bar{t}_1^c = \frac{|j_1^c|}{[|j_1^c| + |j_2^c|]} = \frac{(1 + \Delta t^c)}{2} \quad (3)$$

$$\bar{t}_2^c = \frac{|j_2^c|}{[|j_2^c| + |j_1^c|]} = \frac{(1 - \Delta t^c)}{2} \quad (4)$$

where

$$\Delta t^c = \bar{t}_1^c - \bar{t}_2^c \quad (5)$$

and

$$\bar{t}_1^c + \bar{t}_2^c = 1 \quad (6)$$

Δt^c=difference between counter- and co-ion transport number or membrane permselectivity.

$\bar{t}_1^c$=cation transport number through cation membrane.

$\bar{t}_2^c$=anion transport number through cation membrane and the bar refers to the membrane phase.

Further

$$j_1^c = \bar{t}_1^c(|j_1^c| + |j_2^c|) = \bar{t}_1^c I/F = (1 + \Delta t^c)I/2F \quad (7)$$

$$j_2^c = \bar{t}_2^c(|j_1^c| + |j_2^c|) = \bar{t}_2^c I/F = (1 - \Delta t^c)I/2F \quad (8)$$

(Note: Effective transport numbers are to be distinguished from the usual transport numbers which refer to the above ratios in the absence of concentration gradients [1]).

The brine concentration, c_b, can be obtained from the following material balance (Fig. 1):

$$c_b = \frac{|j_1^c| - |j_1^a|}{|J^c| + |J^a|} = \frac{|j_2^a| - |j_2^c|}{|J^c| + |J^a|} \quad (9)$$

where J^c and J^a are the water fluxes (flows) through the cation and anion membranes, respectively. Consider,

$$c_b = \frac{|j_1^c| - |j_1^a|}{|J^c| + |J^a|} \quad (10)$$

Substitute Eq. (7) into Eq. (10)

$$c_b = \frac{(\bar{t}_1^c I/F) - (\bar{t}_1^a I/F)}{|J^c| + |J^a|} \quad (11)$$

$$= \frac{(1 + \Delta t^c)I/2F - (1 - \Delta t^a)I/2F}{|J^c| + |J^a|} \quad (12)$$

$$= \frac{I/2F[(1 + \Delta t^c) - (1 - \Delta t^a)]}{|J^c| + |J^a|} \quad (13)$$

$$= \frac{I(\Delta t^c + \Delta t^a)}{2F(|J^c| + |J^a|)} \quad (14)$$

$$= \frac{I\overline{\Delta t}}{F(|J^c| + |J^a|)} \quad (15)$$

$$= \frac{I\overline{\Delta t}}{2FJ} \quad (16)$$

$$\overline{\Delta t} = \frac{\Delta t^c + \Delta t^a}{2} \quad (17)$$

$$\text{and } 2J = |J^c| + |J^a| \quad (18)$$

The volume flow through every membrane is equal to the sum of the electro-osmotic and osmotic contributions [2].

Therefore,

$$J = J_{elosm} + J_{osm} \quad (19)$$

The electro-osmotic water flow for the cation and anion membrane is given by [2]:

$$J_{elosm}^c = (\beta_1^c t_1^c - \beta_2^c t_2^c)I \quad (20)$$

$$J_{elosm}^a = (\beta_2^a t_2^a - \beta_1^a t_1^a)I \quad (21)$$

The assumption here is [1] that the electro-osmotic water flow is governed by the drag exerted by the ions. The βs are 'drag' coefficients. They represent the amount of water dragged along with every type of ion by electro-osmosis. For tight membranes, the value of the β should not be very different from the primary hydration water associated with the ions. For porous membranes, however, the value of the β may be several tenfolds larger.

The osmotic contribution is given by [2]:

$$J_{osm} = 2RT\sigma L_p \Delta(gc_s) \quad (22)$$

where R is the universal gas constant, T the absolute temperature, g the osmotic coefficient, σ the reflection coefficient and L_p the hydraulic permeability.

Therefore,

$$J^{c}_{osm} + J^{a}_{osm} = 2RT(g_b c_b - g_f c_f)(\sigma^c L^c_p + \sigma^a L^a_p) \quad (23)$$

Introduction of Eqs. (19)–(21) into Eq. (15) and neglecting the terms $(\beta^c_1 - \beta^c_2)\bar{t}^c_2$ and $(\beta^a_2 - \beta^a_1)\bar{t}^a_1$ in comparison with $\beta^c_1\Delta t^c$ and $\beta^a_2\Delta t^a$, gives: (note: use was made of Eq. (5))

$$c_b = [I(\Delta t^c + \Delta t^a)/2]/[FI(\Delta\beta^c_1\Delta t^c + \beta^a_2\Delta t^a) + 2FRT(g_b c_b - g_f c_f)(\sigma^c L^c_p + \sigma^a L^a_p)] \quad (24)$$

$$= [(\Delta t^c + \Delta t^a)/2]/[F(\beta^c_1\Delta t^c + \beta^a_2\Delta t^a) + 2FRT(g_b c_b - g_f c_f)(\sigma^c L^c_p + \sigma^a L^a_p)/I] \quad (25)$$

Eq. (25) is justified for very permselective membranes where t^c_2 and t^a_1 are small, or where $\beta^c_1 \approx \beta^a_2$ and $\beta^c_2 \approx \beta^a_1$.

For high current densities, the second term (osmotic contribution) in the denominator of Eq. (25) may be neglected.

Therefore,

$$c^{max}_b = \frac{(\Delta t^c + \Delta t^a)/2}{F(\beta^c_1\Delta t^c + \beta^a_2\Delta t^a)} \quad (26)$$

For $\beta^c \approx \beta^a$ and $\Delta t^c \approx \Delta t^a$ (symmetric membranes), Eq. (26) becomes:

$$c^{max}_b = \frac{1}{F(\beta^c_1 + \beta^a_2)} = \frac{1}{2F\beta} \quad (27)$$

where $2\beta = \beta^c_1 + \beta^a_2$, β^c_1 and β^a_2 are the drag coefficients associated with the counter-ions. These coefficients are identical with the electro-osmotic coefficient, $\beta = (J/I)_{\Delta p=\Delta T=0}$ measured at low concentration where co-ion exclusion is practically complete, i.e.

$$t_{\text{counter-ion}} \approx 1,\ t_{\text{co-ion}} \approx 0$$

The cases for which Eq. (27) applies (i.e. for very permselective and/or for approximately symmetric membranes, at high current densities) are of considerable interest and importance [2] since the brine concentration depends only on the electro-osmotic coefficients, β^c_1 and β^a_2. c^{max}_b can also be determined from Eqs. (25)–(27).

$$c_b = \frac{I\overline{\Delta t}}{F(J_{elosm} + J_{osm})} \quad (28)$$

$$= \frac{I\overline{\Delta t}}{FJ_{elosm}(1 + J_{osm}/J_{elosm})} \quad (29)$$

$$= \frac{c^{max}_b}{1 + J_{osm}/J_{elosm}} \quad (30)$$

2.2. Symmetric cells

The theory of EOP, in general, leads to difficult computations which must be carried out numerically according to Garza [1]. However, there is one case in which results can be given in terms of simple closed formula. This case depends on the assumption of a symmetric cell [1]. In a symmetric cell the cation- and anion-exchange membranes have identical physical properties in all regards except for the sign of their fixed charges. Because of cell symmetry, the magnitudes of the counter-ion fluxes through both membranes are the same. When a symmetric salt is chosen like potassium chloride, the anion and cation have equal mobilities. In other words, the magnitude of the cation flux through the cation-exchange membrane is the same as the magnitude of the anion flux through the anion-exchange membrane. Also the magnitude of the co-ion fluxes through both membranes are the same, i.e. the magnitude of the anion flux through the cation-exchange membrane is the same as the magnitude of the cation flux through the anion-exchange membrane.

$$|j^c_i| = |j^a_2|;\ |j^a_1| = |j^c_2| \quad (31)$$

and thus

$$\bar{t}^c_1 = \bar{t}^a_2;\ \bar{t}^a_1 = \bar{t}^c_2;\ \Delta t^c = \Delta t^a = \overline{\Delta t} \quad (32)$$

Water flows are also of equal magnitude and opposite direction:

$$|J^c| = |J^a| = J \text{ or } J^c = -J^a = J \quad (33)$$

The amount of salt leaving through the brine outlet per unit time and membrane area, $2Jc_b$, is related to the cation flows by Eqs. (9) and (18):

$$2Jc_b = |j^c_i| - |j^a_1| \quad (34)$$

and in the symmetric system is:

$$J = I\overline{\Delta t}/2c_bF \quad (35)$$

2.2.1. Current efficiency

The amount of salt transferred per Faraday of current passed through a symmetric unit cell is given from Eq. (35) by [1]:

$$\varepsilon_p = \frac{2Jc_b}{I/F} = \overline{\Delta t} \quad (36)$$

The overall efficiency, ε, is however, somewhat smaller than ε_p, since hydrated water is also lost with the salt. The effective current density, i.e. the purification of the product achieved, is given by [1]:

$$I_{eff} = F(\frac{Q}{A_m} - 2J)(c_f - c_p) = F(\frac{Q}{A_m} - 2J)(\Lambda c_f) \quad (37)$$

where Q is the amount of feed solution entering a channel per unit time, A_m the effective membrane area (Fig. 1), Λ the degree of mineralization given by [1]:

$$\Lambda = \frac{c_f - c_p}{c_f} \quad (38)$$

where c_f is the concentration of the feed solution entering the stack, and c_p the concentration of the product leaving it.

The mass balance for the salt is:

$$\frac{Qc_f}{A_m} = (\frac{Q}{A_m} - 2J)c_p + 2Jc_b \quad (39)$$

Therefore,

$$\frac{I_{eff}}{F} = (\frac{Q}{A_m} - 2J)(c_f - c_p) = 2J(c_b - c_f) \quad (40)$$

and

$$\varepsilon = \frac{I_{eff}}{I} = \Delta t(1 - \frac{c_f}{c_b}) = \varepsilon_p \cdot \varepsilon_w \quad (41)$$

where

$$\varepsilon_w = 1 - c_f/c_b \quad (42)$$

The overall efficiency in ED is presented as the product of two terms, one due to the lack of ideal permselectivity in the membranes, ε_p, the other reflecting the loss of water to the brine, ε_w.

2.2.2. Electro-osmotic flow

Electro-osmotic flow is measured under the restrictions [1]:

$$\Delta c = 0,\ d\mu_w/dx = 0$$

Under these conditions are:

$$J_{elosm} = (j_1\beta_1 + j_2\beta_2)F \quad (43)$$

Eq. (43) can also be written as:

$$J_{elsom} = (\beta_1 t_1 - \beta_2 t_2)I \quad (44)$$

$$= [\beta_1(t_1 - t_2) + (\beta_1 - \beta_2)t_2]I \quad (45)$$

$$= [\beta_1\Delta t + (\beta_1 - \beta_2)t_2]I \quad (46)$$

For small values of t_2, or for $\beta_1=\beta_2=\beta$, Eq. (46) becomes:

$$J_{elsom} = \beta^\circ \Delta t I \quad (47)$$

where β° is the customary electro-osmotic coefficient measured at low ionic strength where co-ion exclusion is high and $\Delta t \approx 1$, i.e.:

$$\beta^\circ = (J/I)_{\Delta c=\Delta p=\Delta T=0,\ \Delta t=1} = (J_{elosm}/I)_{\Delta t=1}$$

2.2.3. Osmotic flow at high co-ion exclusion

Osmotic flow is measured under the restrictions [1]:

$$I = \Delta p = 0,\ j_1 = j_2 = 0$$

(absence of electric current, hydrostatic pressure and impermeable solutes). In this case is [1]:

$$J_{osm} = L_p\sigma\Delta\pi \quad (48)$$

2.2.4. Volume flow in electro-osmotic pumping

The volume flow into the membrane concentrating cells in EOP is the sum of the electro-osmotic and osmotic water flows and is given by [1]:

$$J = -L_p\sigma\Delta\pi + \beta^\circ\Delta t I \quad (49)$$

3. Experimental

3.1. Membranes

The membrane and membrane types shown in Table 1 were selected for the EOP study of sodium chloride solutions [6]. However, only results of the

Table 1
Membrane and membrane types selected for EOP of sodium chloride solutions

Membranes	Anionic (A) and cationic (C)	Type
Selemion AMV	A	Homogeneous
Selemion CMV	C	Homogeneous
Ionac MA 3470	A	Heterogeneous
Ionac MC 3475	C	Heterogeneous
Raipore R4030	A	Homogeneous
Raipore R4010	C	Homogeneous
Ionics A 204 UZL 386	A	Homogeneous
Ionics C 61 CZL 386	C	Homogeneous
WTPS A-1	A	Heterogeneous
WTPS C-1	C	Heterogeneous
WTPVC A-2	A	Heterogeneous
WTPVC C-2	C	Heterogeneous
WTPST A-3	A	Heterogeneous
WTPST C-3	C	Heterogeneous

WTPS: Watertek polysulphone.
WTPVC: Watertek polyvinyl chloride.
WTPST: Watertek polystyrene.

Selemion AMV and CMV membranes will be presented here.

3.2. Unit-cell construction

A unit cell can be constructed in the following number of ways [1]:

1. Glueing the membrane edges together with a suitable glue;
2. Glueing the membrane edges to either side of an injection moulded nylon ring (Fig. 2) which has a brine exit within it; and
3. Mounting of the membranes between gaskets as in the filter press stack design.

For experiment, however, the volume of the brine compartment must be kept to a minimum in order to minimize time for achieving the steady state and for beginning to measure water flow. An injection moulded nylon ring (Fig. 2) was used in the EOP experiments as the unit cell.

3.3. Determination of brine concentration, current efficiency and water flow as a function of feed concentration and current density

The EOP cell used in the experiments was described by Oren and Litan [7] and is shown in Fig. 3. It

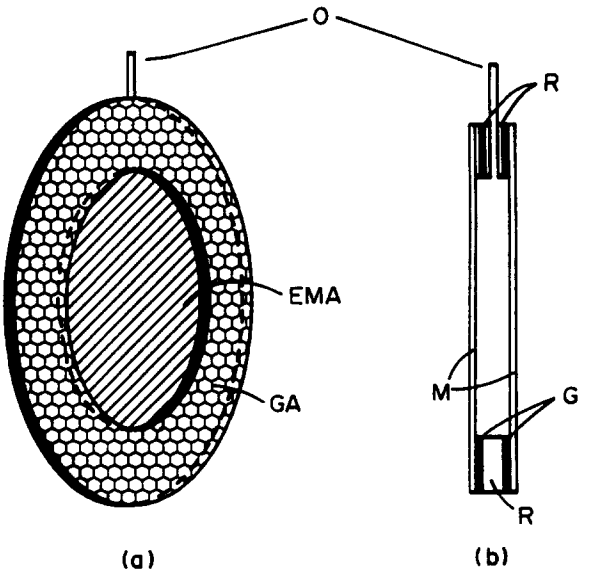

Fig. 2. Schematic diagram of injection moulded nylon ring that was used for construction of the membrane bag. The membranes are glued to both sides of the ring. (a) Front view; (b) Lateral view; o: Brine outlet; EMA: Effective membrane area; GA: Glueing area; M: Membrane; G: Glue; R: Nylon ring.

consists of two symmetric units, each of which contains a separate electrode. A carbon slurry was circulated through the electrode compartments and was used as electrode rinse solution. The membranes were attached to the nylon ring with silicon sealant and the nylon ring (membrane bag) was placed between the two circulating cells and rubber rings were used to secure sealing. Approximately 40 l of solution containing salt was circulated through the cell renewing its content ≈60 times per minute. In this way an approximately constant feed concentration was maintained during the experiments.

Efficient stirring and streaming of the solution in the cell were affected by the Meares and Sutton's method of forcing the solution onto the membrane surface through perforated polypropylene discs [7]. This has been shown to be a very efficient way of stirring. Constant current was applied to the cell by a Hewlett–Packard constant current source. Current was measured with a Hewlett–Packard digital multimeter. Brine samples were collected at certain intervals and their volume and concentration determined. Each point on the plots of c_b vs. I, and

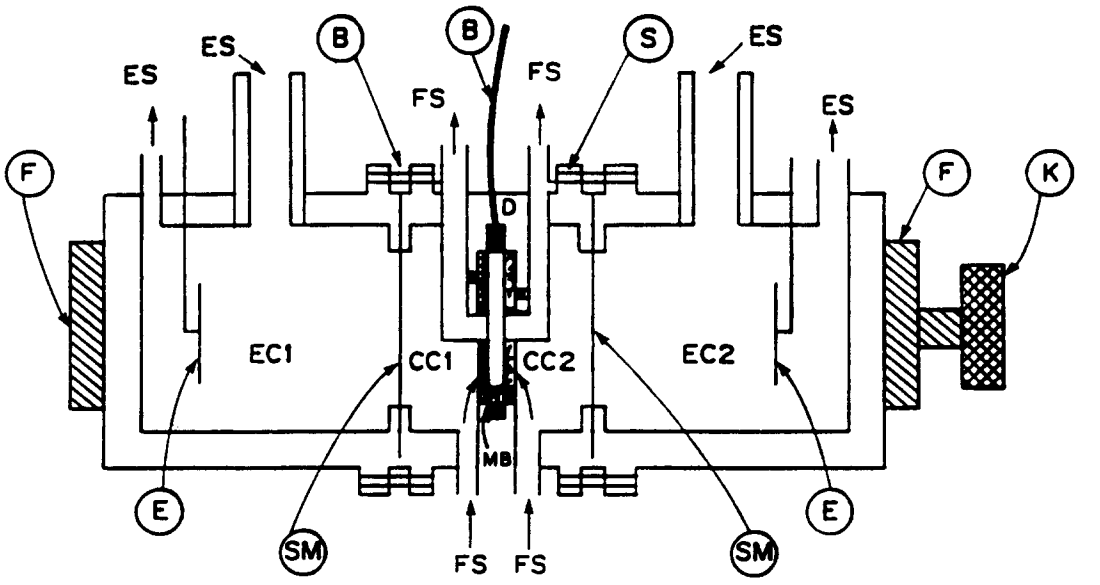

Fig. 3. Schematic diagram of the apparatus used for the EOP experiments. EC1 and EC2: Electrode cells; CC1 and CC2: Circulation cells for the feed solution (FS); B: Brine outlet; MB: Membrane bag; SM: Membrane separating the electrode compartments from the feed solution; E: Electrodes; D: Perforated porous polypropylene disks; S: Stainless steel screws; F: Clamping frame; and K: Tightening knob.

of J vs. I_{eff} was the average of 3 to 5 measurements after the system had reached the stationary state (from 3 to 6 h). Concentration changes in the feed solution during the time of the experiments were found to be negligible.

Current efficiency, ε_p, was calculated as follow [1]:

$$\varepsilon_p = \frac{2Jc_b}{I/F} = \frac{c_b(V/t)}{I/F} \equiv \overline{\Delta t} \tag{50}$$

where c_b represents brine concentration, V the volume of the solution that enters the bag per unit area (7.55 cm^2) in t seconds ($V/t=2J$), I the applied current density (mA/cm^2) and F the Faraday constant.

The maximum brine concentration, c_b^{max}, was determined from the following relationship [1]:

$$c_b^{max} = \frac{1}{2\beta F} \tag{51}$$

where 2β is the electro-osmotic coefficient determined from the slope of the J vs. I_{eff} plots (see Appendix A and Fig. 15).

3.4. Membrane potential

The difference between the counter- and co-ion transport number, Δt, which is called the apparent transport number or membrane permselectivity, was measured as follows:

The potential ($\Delta\psi_m$) of a membrane is usually measured between 0.1/0.2 mol/l (5.85/11.7 g/l) or 0.5/1.0 mol/l (29.25/58.5 g/l) sodium chloride solutions in a specially designed cell with calomel electrodes [8]. The theoretical potential, $\Delta\psi_i$, is calculated from the activities of the two solutions. Membrane permselectivity, Δt, can then be calculated from these values where ($\Delta\psi_m$) is the measured potential and a_s''/a_s' is the ratio of the salt activities on both sides of the membrane [6].

$$\Delta t = \frac{\Delta\psi_m}{\Delta\psi_i} \tag{52}$$

where $\Delta t = 2t_1 - 1$ and

$$\Delta\psi_i = \frac{RT}{F}\ln\frac{a_s''}{a_s'} \tag{53}$$

4. Results and discussion

4.1. Electro-osmotic pumping of sodium chloride solutions using Selemion AMV and CMV membranes

Brine concentration, water flows and current efficiencies were determined at different current densities for different sodium chloride feed water concentrations. Membrane permselectivities (apparent transport numbers – Δt's) were measured at the same concentration differences as encountered during EOP experiments when brine concentration had reached the steady state (3 to 5 h). A typical example of EOP results is shown in Appendix A [6].

4.1.1. Brine concentration

Brine concentration (c_b) as a function of current density (I) is shown in Fig. 4. Brine concentration increases rapidly in the beginning of the run and then levels off at higher current densities. Brine concentration increases with increasing current density and feed water concentration. The brine concentrations obtained at the highest current densities used are shown in Table 2. Brine concentrations between 19.3 and 29.8% (193 and 298 g/l) were obtained between 0.05 and 1.0 mol/l (2.925 and 58.5 g/l) feed concentration range.

Table 2
Brine concentration obtained at the highest current densities for different sodium chloride feed concentrations

Feed concentration (mol/l)	Brine concentration (%) Selemion AMV and CMV
0.05	19.3
0.10	25.1
0.50	27.2
1.0	29.8

It further appears that brine concentration will reach a maximum value, c_b^{max} (Fig. 4) in the 0.1 to 1.0 mol/l feed concentration range at high current densities. Maximum brine concentration, c_b^{max}, was calculated from the following two relationships, viz.

$$c_b^{max} = \frac{1}{2\beta F} \quad \text{(see Eq. (27))}$$

and

$$c_b^{max} = c_b(1 + J_{osm}/J_{elosm})$$

(see Appendix A and Eq. (30)).

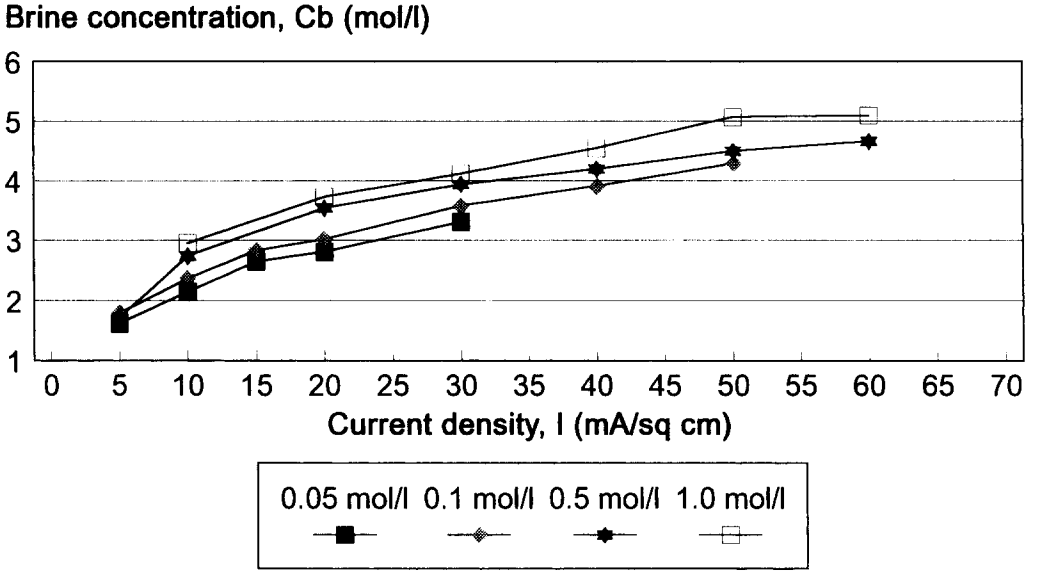

Fig. 4. Brine concentration as a function of current density for four different NaCl feed concentrations. Selemion AMV and CMV membranes.

Table 3
Maximum brine concentration calculated from $c_b^{max} = 1/2F\beta$ [a] and $c_b^{max} = c_b(1 + J_{osm}/J_{elosm})$ [b] for Selemion AMV and CMV membranes

Feed concentration (mol/l)	Maximum brine concentration, c_b^{max} (mol/l)	
	1 [c]	2 [d]
0.05	4.55	4.54
0.10	5.05	5.06
0.50	5.36	5.31
1.00	6.48	6.49

[a] Calculated from electro-osmotic coefficients [6] (see Appendix A).
[b] Calculated from $J_{elosm} = J - J_{osm}$ (y-intercept and the corresponding c_b values) [6] (see Appendix A).
[c] $c_b^{max} = 1/2F\beta$ (Eq. (27)).
[d] $c_b^{max} = c_b(1 + J_{osm}/J_{elosm})$. (eq. (30)).

The results are shown in Table 3. Extremely good correlations were obtained with the above two relationships to determine c_b^{max}. Consequently, any one of these two methods can be used to determine c_b^{max}.

Maximum brine concentration seems to depend more on feed concentration (Table 3). Maximum brine concentration that can be obtained increases with increasing feed concentration.

Brine concentrations at different current densities were calculated from measured transport numbers and volume flows (J) with the relationship:

$$c_b = \frac{I\overline{\Delta t}}{2FJ} \quad \text{(see Eq. (16))}$$

Experimental and calculated brine concentrations are shown in Figs. 5–8. The correlation between the calculated and experimentally determined brine concentrations expressed as the ratio $c_{b\ calc}/c_{b\ exp}$ is shown in Table 4. The calculated brine concentrations were higher than the experimentally determined brine concentrations in the 0.05 to 0.1 mol/l feed concentration range (Figs. 5 and 6 and Table 4). However, calculated brine concentration became lower than the experimentally determined brine concentrations in the 0.5 to 1.0 mol/l feed concentration range (Figs. 7 and 8 and Table 4).

Good correlations were obtained between the calculated and experimentally determined brine concentrations depending on the feed concentration and current density used (Table 4). The ratio $c_{b\ calc}/c_{b\ exp}$ varied between 1.0 and 1.11 from 10 to 50 mA/cm^2 (0.1 mol/l feed) current density range. However, poorer correlations were obtained at lower (0.05 mol/l) and higher (0.5 and 1.0 mol/l) feed concentrations (Table 4). The ratio $c_{b\ calc}/c_{b\ exp}$ varied between 1.28 and 1.22 at 0.05 mol/l feed (10 to 30 mA/cm^2 current density range) and between 0.85 and 0.78 and between 0.82 and 0.73 at feed concentrations of 0.5 and 1.0 mol/l, respectively (10 to 50 mA/cm^2 current density range). Therefore, it appears that brine concentration should be predicted with an accuracy of ≈10% from simple transport number and water flow determinations when the feed water concentration is 0.1 mol/l. However, less accurate predictions will be possible when the feed water concentration is lower (0.05 mol/l) and higher (0.5 to 1.0 mol/l).

4.1.2. Current efficiency

Current efficiency (ε_p) determined during the EOP experiments as a function of current density is shown in Fig. 9. Current efficiency increases with increasing feed water concentration in the 0.05 to 1.0 mol/l range. However, current efficiency was slightly lower at the highest feed concentration (Fig. 9).

No significant change in the current efficiency was observed as a function of current density in the feed concentration range studied (Fig. 9). This showed that the limiting current density was not reached in the range of current densities and feed water concentrations used.

The apparent transport numbers for a membrane pair ($\overline{\Delta t}$), for the anion (Δt^a) and cation (Δt^c) membranes determined from membrane potential measurements (see Eq. (52)) for a concentration difference similar to that obtained in the EOP experiments at the different current densities and feed water concentrations used, are shown in Figs. 10–13. The current efficiencies (ε_p) as determined by the EOP method shown in Fig. 9, are also shown in Figs. 10–13. The correlation between the apparent transport numbers ($\overline{\Delta t}$, Δt^a, Δt^c) and the current efficiency (ε_p) is shown in Table 5.

The apparent transport numbers ($\overline{\Delta t}$, Δt^a, Δt^c) were higher than the current efficiencies at the lower feed water concentrations (0.05 to 0.1 mol/l) (Figs. 10

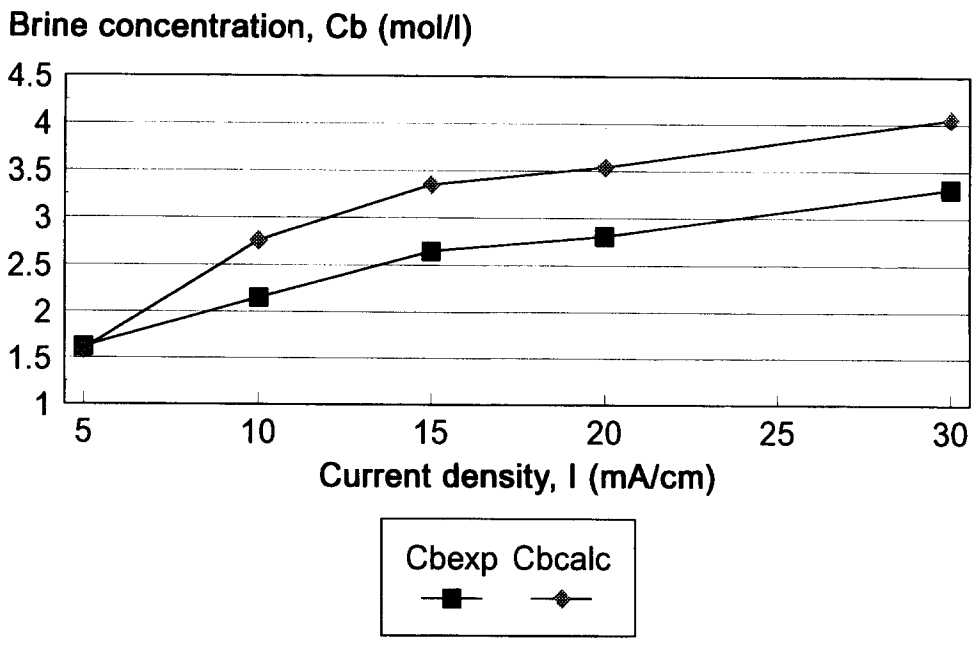

Fig. 5. Experimental and calculated brine concentrations as a function of current density for 0.05 mol/l NaCl feed solution. Selemion AMV and CMV membranes.

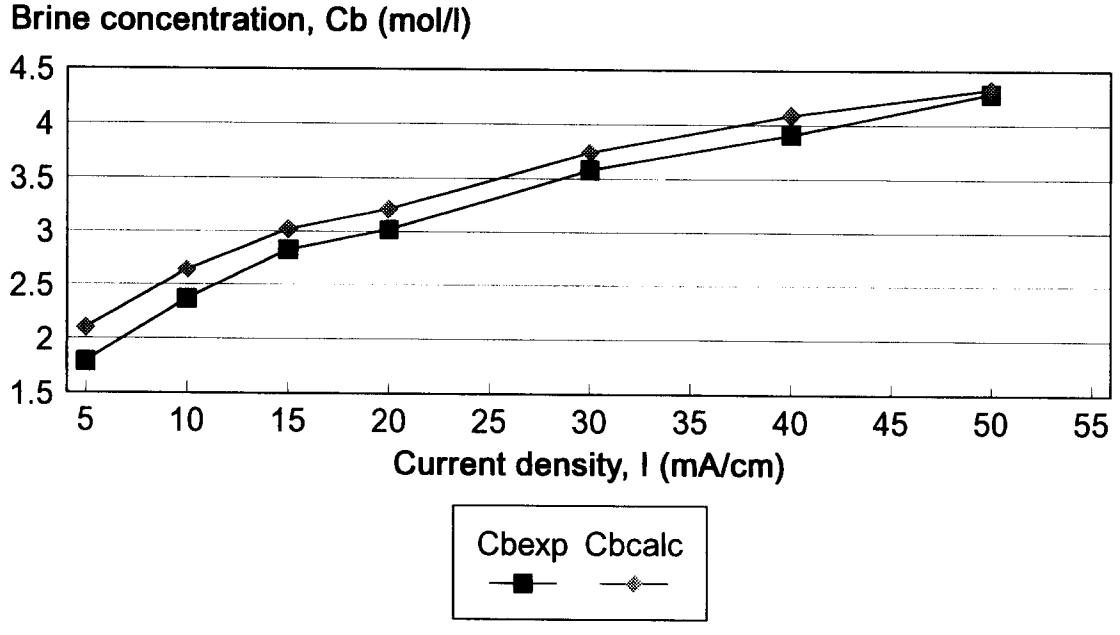

Fig. 6. Experimental and calculated brine concentrations as a function of current density for 0.1 mol/l NaCl feed solution. Selemion AMV and CMV membranes.

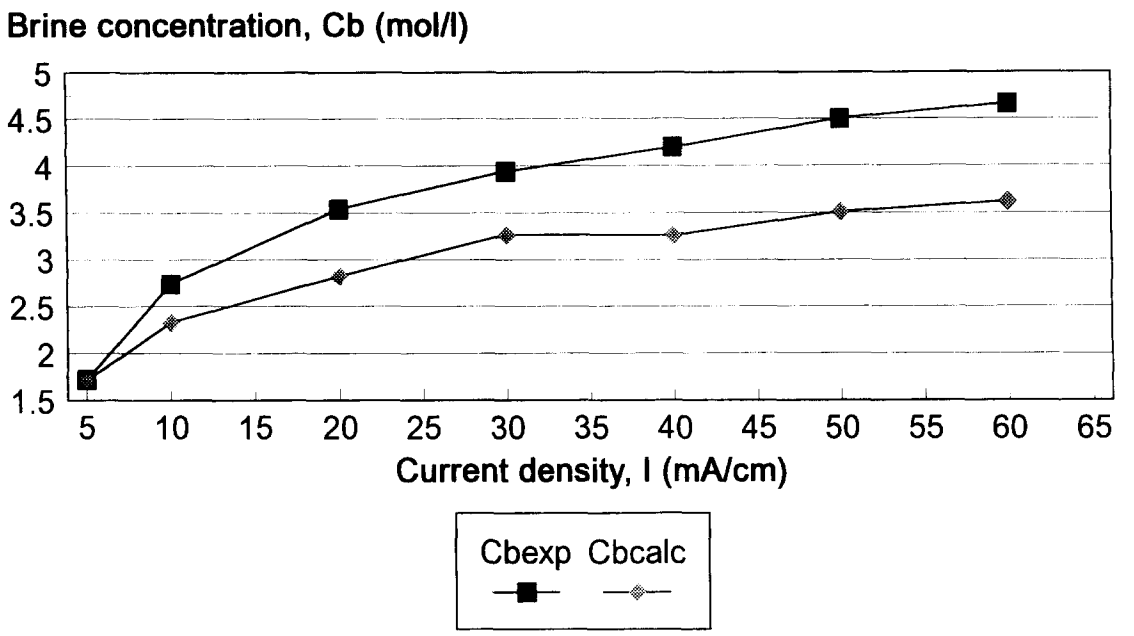

Fig. 7. Experimental and calculated brine concentrations as a function of current density for 0.5 mol/l NaCl feed solution. Selemion AMV and CMV membranes.

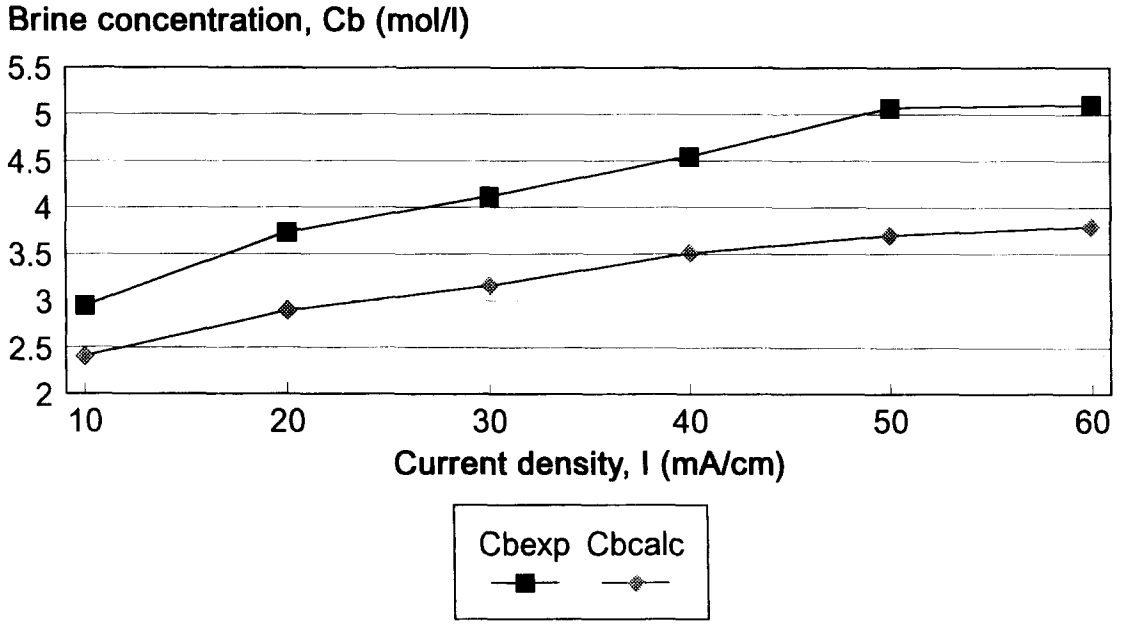

Fig. 8. Experimental and calculated brine concentrations as a function of current density for 1.0 mol/l NaCl feed solution. Selemion AMV and CMV membranes.

Table 4
Correlation between calculated ($c_{b\ calc}$) and experimentally ($c_{b\ exp}$) determined brine concentrations for Selemion AMV and CMV membranes

Current density (mA/cm^2)	$c_{b\ calc}/c_{b\ exp}$			
	Concentration (mol/l)			
	0.05	0.1	0.5	1.0
5	0.98	1.17	0.99	
10	1.28	1.11	0.85	0.82
15	1.26	1.07		
20	1.26	1.06	0.79	0.78
25				
30	1.22	1.04	0.83	0.77
40		1.05	0.77	0.77
50		1.00	0.78	0.73
60			0.77	0.74

and 11 and Table 5). However, the apparent transport numbers became smaller than the current efficiencies at the higher feed water concentrations (0.5 to 1.0 mol/l) (Figs. 12 and 13 and Table 5).

Good correlations were obtained between the apparent transport number of a membrane pair $\overline{\Delta t}$ and current efficiency (ε_p) depending on the feed concentration and current density used (Table 5). The ratio between $\overline{\Delta t}/\varepsilon_p$ varied between 1.01 and 1.13 from 10 to 50 mA/cm^2 (0.1 mol/l feed) current density range. However, poorer correlations were obtained at lower (0.05 mol/l) and higher (0.5 and 1.0 mol/l) feed concentrations. The ratio $\overline{\Delta t}/\varepsilon_p$ varied between 1.28 and 1.23 at 0.05 mol/l feed concentration from 0 to 30 mA/cm^2 current density range. The ratio $\overline{\Delta t}/\varepsilon_p$ varied between 0.82 and 0.78 at 0.5 mol/l feed concentration and the same ratio varied between 0.82 and 0.73 at 1.0 mol/l feed concentration (current density range from 10 to 50 mA/cm^2). Therefore, it appears that apparent transport numbers determined from a simple membrane potential method should give a good approximate estimation of membrane performance for ED concentration/desalination applications depending on the feed concentration and current density used. Membrane performance for concentration/desalination applications should be predicted with an accuracy of ≈10% from membrane potential measurements when the feed concentration is 0.1 mol/l. The apparent transport numbers

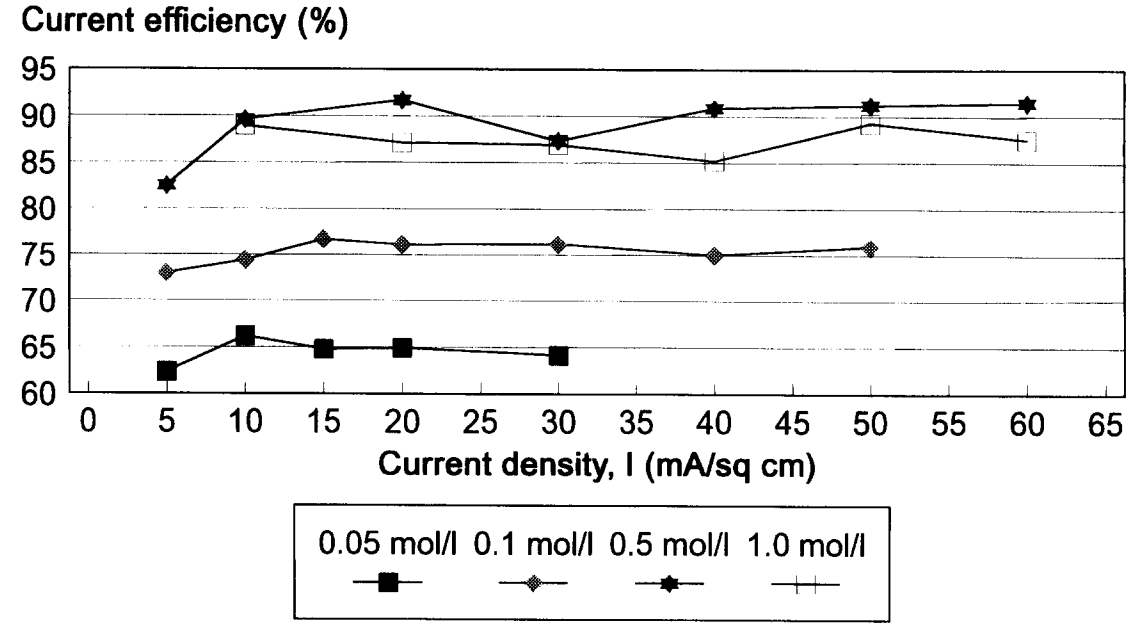

Fig. 9. Current efficiency (ε_p) as a function of current density for four different NaCl feed concentrations. Selemion AMV and CMV membranes.

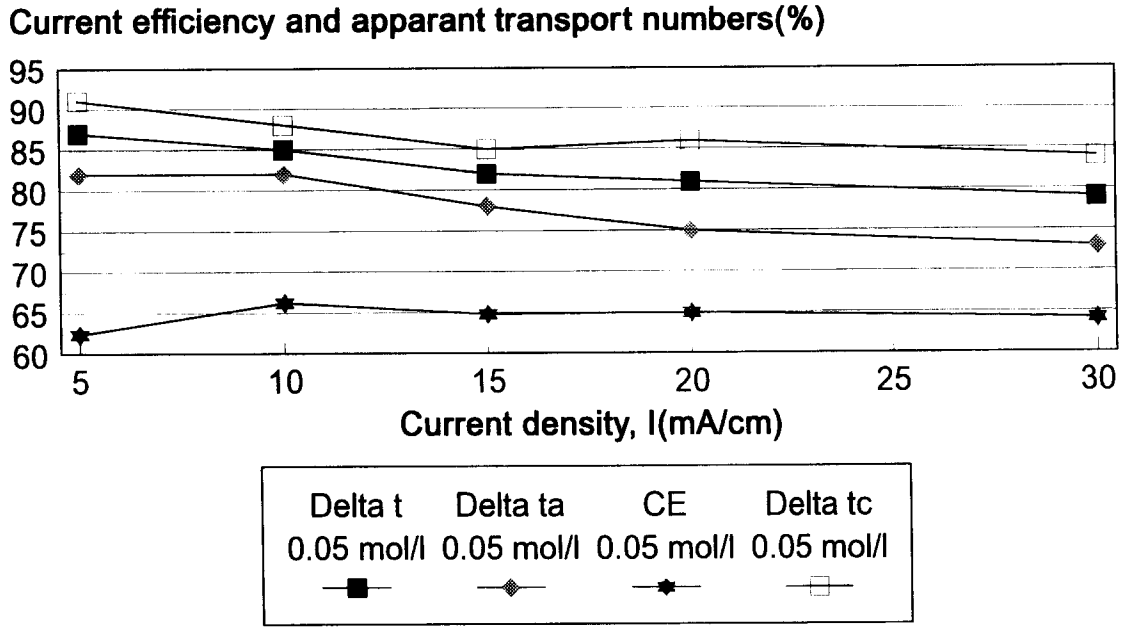

Fig. 10. Current efficiency (CE=ε_p) and apparent transport numbers, ($\overline{\Delta t}$, Δt^a, Δt^c), as a function of current density for 0.05 mol/l NaCl feed. Selemion AMV and CMV membranes. Delta t=$\overline{\Delta t}$; Delta ta=Δt^a; Delta tc=Δt^c.

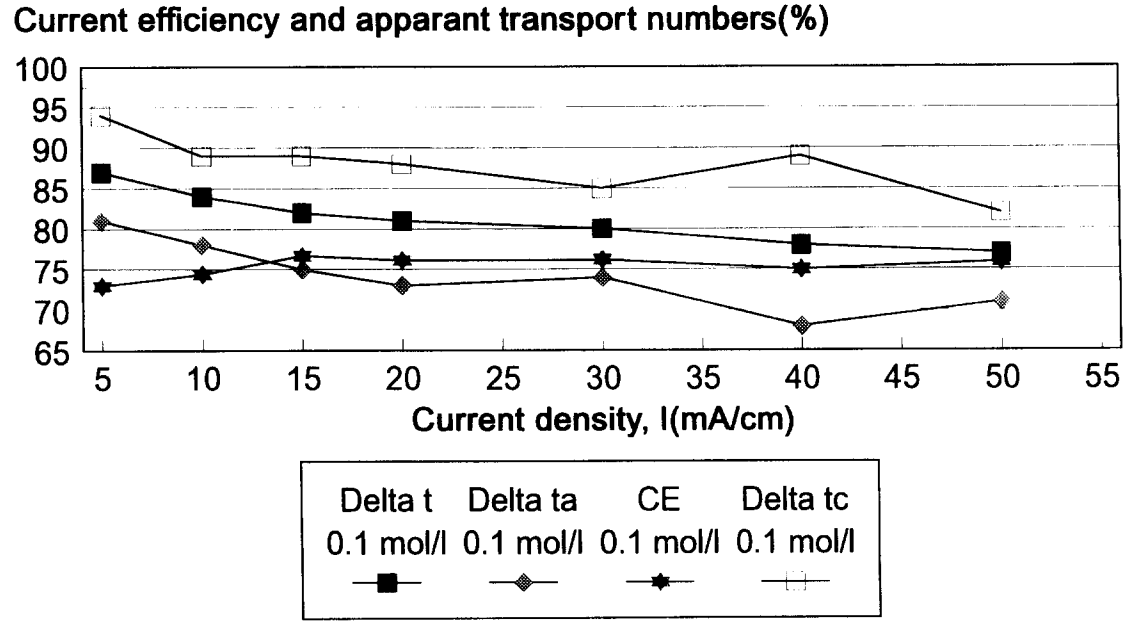

Fig. 11. Current efficiency (CE=ε_p) and apparent transport numbers ($\overline{\Delta t}$, Δt^a, Δt^c), as a function of current density for 0.1 mol/l NaCl feed. Selemion AMV and CMV membranes. Delta t=$\overline{\Delta t}$; Delta ta=Δt^a; Delta tc=Δt^c.

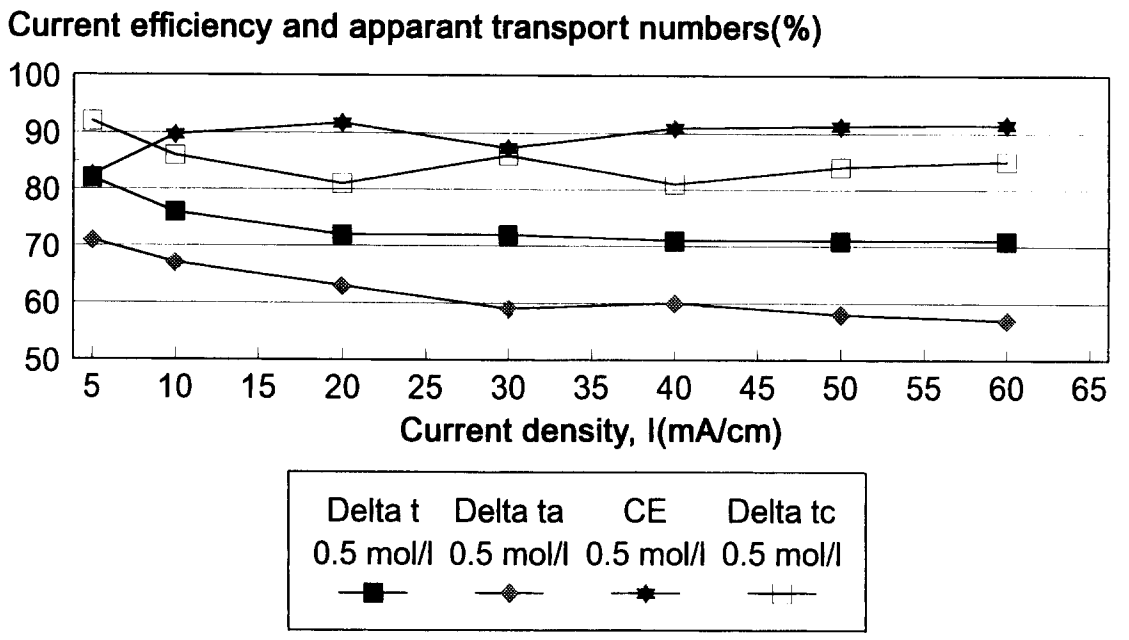

Fig. 12. Current efficiency (CE $=\varepsilon_p$) and apparent transport numbers ($\overline{\Delta t}$, Δt^a, Δt^c) as a function of current density for 0.5 mol/l NaCl feed Selemion AMV and CMV membranes. Delta t=$\overline{\Delta t}$; Delta ta=Δt^a; Delta tc=Δt^c.

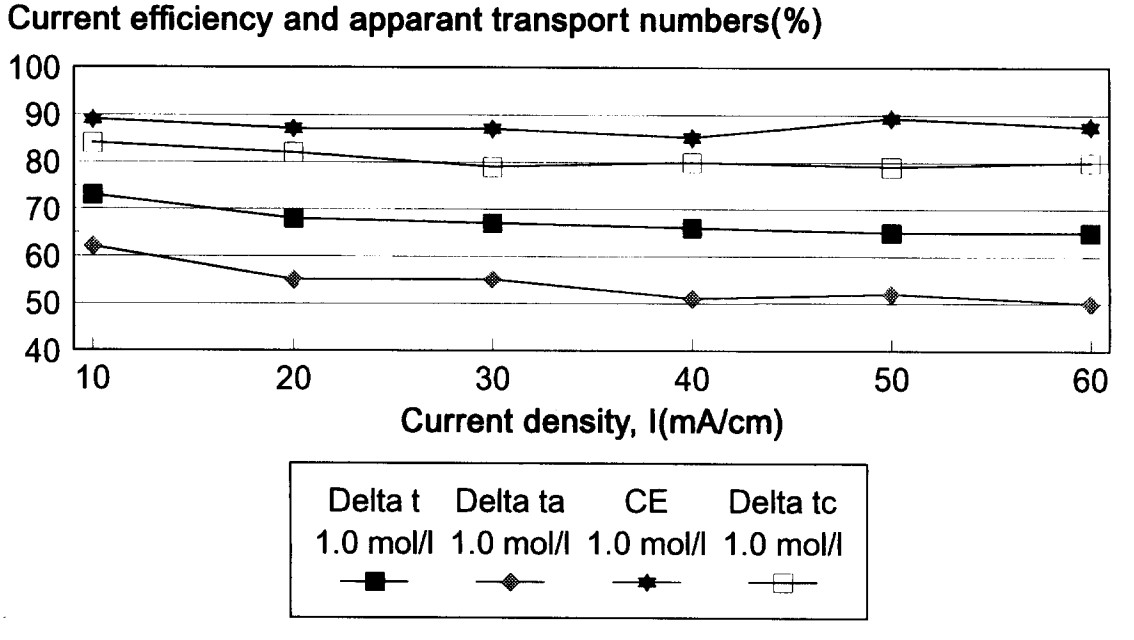

Fig. 13. Current efficiency (CE=ε_p) and apparent transport numbers ($\overline{\Delta t}$, Δt^a, Δt^c) as a function of current density for 1.0 mol/l NaCl feed. Selemion AMV and CMV membranes. Delta t=$\overline{\Delta t}$; Delta ta=Δt^a; Delta tc=Δt^c.

Table 5
Correlation between apparent transport number for a membrane pair ($\overline{\Delta t}$) and current efficiency (ε_p) for Selemion AMV and CMV membranes

Current density (mA/cm^2)	$\overline{\Delta t}/\varepsilon_p$			
	Concentration (mol/l)			
	0.05	0.1	0.5	1.0
5	1.39	1.19	0.99	
10	1.28	1.13	0.82	0.82
15	1.27	1.07		
20	1.25	1.06	0.79	0.78
25				
30	1.23	1.05	0.82	0.77
40		1.04	0.78	0.77
50		1.01	0.78	0.73
60			0.78	0.74

Table 6
Water flow (J_i) through the Selemion AMV and CMV membranes relative to the flow at $J_{0.5}$ mol/l or $J_{0.1}$ mol/l

Current density (mA/cm^2)	$J_i/J_{0.5}$ mol/l and ($J_i/J_{0.1}$ mol/l)			
	Concentration (mol/l)			
	0.05	0.1	0.5	1.0
5	1.14 (1.34)	0.85 (1.0)	1.0	
10	0.94 (0.97)	0.97 (1.0)	1.0	0.93
15	(0.90)	(1.0)	1.0	
20	0.89 (0.90)	0.99 (1.0)	1.0	0.92
25			1.0	
30	0.88 (0.91)	0.96 (1.0)	1.0	0.95
40		0.89	1.0	0.86
50		0.87	1.0	0.87
60			1.0	0.87

i=0.05; 0.1; 0.5 and 1.0 mol/l.

of the anion (Δt^a) and the cation (Δt^c) membranes may also be used to predict approximate performance for concentration/desalination applications at this feed concentration (Fig. 11 and Table 5). However, much poorer correlations between $\overline{\Delta t}$ and ε_p were obtained at lower (0.05 mol/l) and higher (0.5 and 1.0 mol/l) feed concentrations (Table 5). It appears that it should not be possible to predict membrane performance with an accuracy of more than 20% at these feed concentration levels.

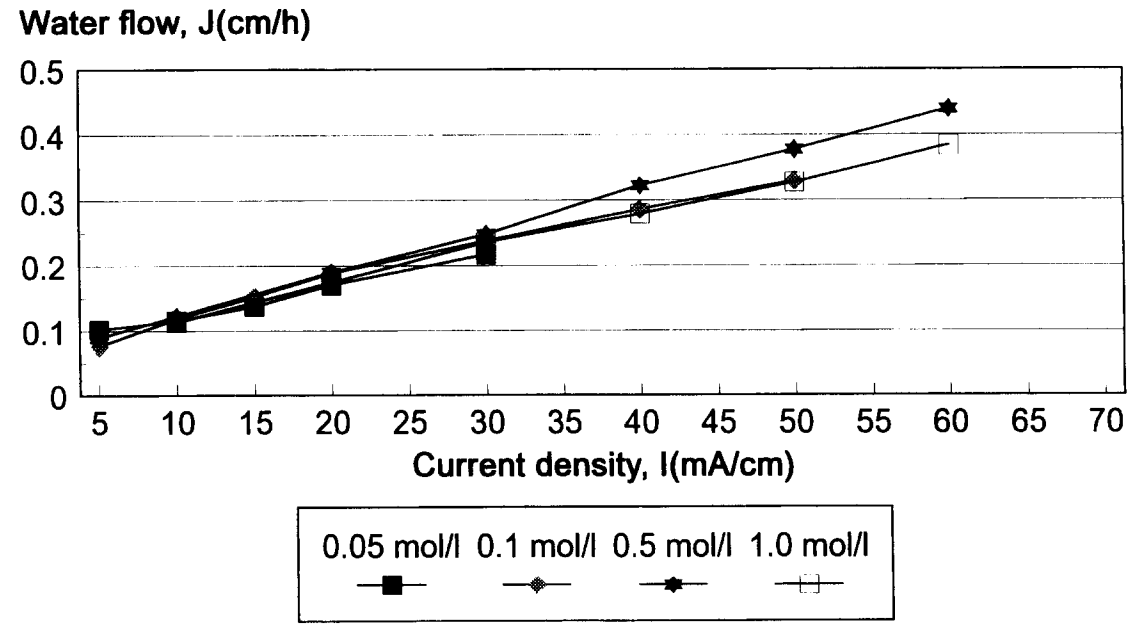

Fig. 14. Water flow through the Selemion AMV and CMV membranes as a function of current density and feed water concentration.

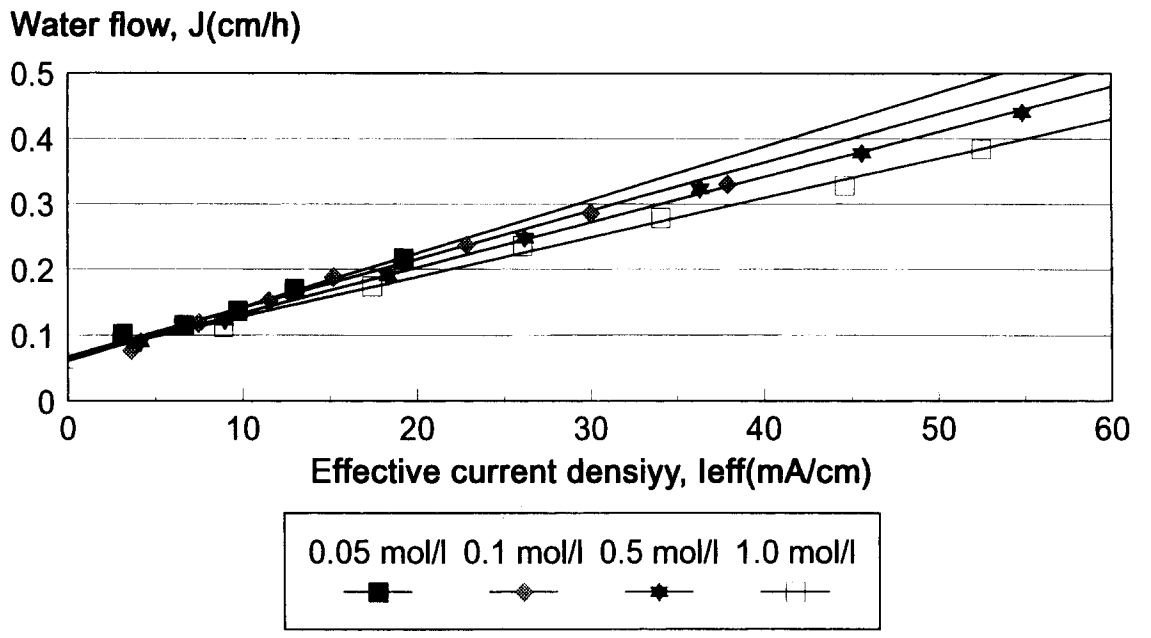

Fig. 15. Water flow through the Selemion AMV and CMV membranes as a function of effective current density and feed water concentration.

4.1.3. Water flow

Water flow (J) through the membranes as a function of current density and feed water concentration is shown in Fig. 14 and Table 6. Water or volume flow through the membranes increases as a function of both current density and feed water concentration (Fig. 9). However, water flow was lower at the highest feed concentration (1.0 mol/l). It is interesting to note that the current efficiency has been slightly lower at the highest feed water concentration (1.0 mol/l) than at the second highest feed concentration (0.5 mol/l). Therefore, it appears that increasing current efficiency is caused by an increasing water flow through the membranes.

Water flow (J) through the membranes as a function of effective current density, I_{eff}, (actual current density times Coulomb efficiency) and feed water concentration are shown in Fig. 15. Straight lines were obtained at higher values of I_{eff}. The slope of these lines corresponds to the combined electro-osmotic coefficient (2β) of a membrane pair. The electro-osmotic coefficients decreases significantly with increasing feed concentration (Fig. 15) as can be seen from the slopes of the lines [6].

The electro-osmotic coefficients as a function of feed concentration are shown in Table 7. The reduction in the electro-osmotic coefficients with increasing feed concentration can be ascribed to deswelling of the membranes as high feed concentration [9,10] and/or a reduction in membrane permselectivity at high feed concentration [11].

Table 7
Effect of feed concentration on the electro-osmotic coefficient (EOC) [a]; the maximum salt brine concentration, c_b^{max}, and on the water passed through the membranes (Selemion AMV and CMV)

Feed concentration (mol/l)	EOC (l/F)	c_b^{max} (mol/l)	mol H_2O/ Faraday
0.05	0.219	4.55	12.2
0.10	0.198	5.05	11.0
0.5	0.187	5.36	10.4
1.0	0.154	6.48	8.6

[a] See Appendix A.

The effect of the electro-osmotic coefficient on the maximum brine concentration, c_b^{max}, is also shown in Table 7. Maximum brine concentration increases with decreasing electro-osmotic coefficients.

Approximately 9 to 12 mol H_2O/Faraday was passed through the membranes in the 0.05 to 1.0 mol/l feed concentration range (Table 7). Less water was passed through the membranes with increasing feed water concentration.

Table 8
Osmotic flow [a] (J_{osm}) relative to the total flow (J) through the Selemion AMV and CMV membranes as a function of current density

Current density (mA/cm^2)	Osmotic flow relative to total flow J_{osm}/J (%)			
	Feed concentration (mol/l)			
	0.05	0.1	0.5	1.0
10	52.3	57.4	51.2	69.9
20	35.4	36.0	32.8	45.4
30	27.7	28.4		33.5
40			19.3	28.3
50		20.5		
60			14.1	20.6

[a] See Appendix A.

The osmotic flow (J_{osm}) relative to the total flow (J) through the membranes as a function of current density, is shown in Table 8. Osmotic flow decreases with increasing current density in the 0.05 to 1.0 mol/l feed concentration range. The contribution of osmotic flow at a current density of 20 mA/cm^2 (0.1 mol/l feed) for example was 36.4% of the total flow through the membranes. Consequently, osmosis contributes significantly to water flow through the membranes especially at relatively low current density. The osmotic flow contribution to total water flow through the membranes was much less at high current density. Osmotic flow contribution to total flow through the membranes at a current density of 50 mA/cm^2 (0.1 mol/l feed) was 20.5%. Similar results were obtained at other feed concentrations.

4.1.4. Discrepancy between transport numbers derived from potential measurements and current efficiency actually obtained.

The correct relationships to be used when measuring membrane potential for the prediction of desalting in ED, are as follows [6]:

$$[J/I]_{\Delta\mu_s; J_v=0} = \Delta t/F \tag{54}$$

and

$$\Delta t/F = -[\Delta\psi/\Delta\mu_s]_{I=0; J_v=0} \tag{55}$$

The correct Onsager relationship for potential measurement is at zero current and zero volume flow, and for the transport number, at zero concentration gradient and zero volume flow [6]. In practical, ED measurements are conducted at zero pressure and in the presence of concentration gradients and volume flows. These factors will influence the results considerably in all systems in which volume flow is important and where the concentration factor is high as is encountered in EOP. In the measurement of membrane potential, the volume flow is against the concentration potential and in general will decrease potential. In ED, water flows help to increase current efficiency, but the concentration gradient acts against current efficiency.

In the case of sodium chloride solutions, the apparent transport number of the membrane pair ($\overline{\Delta t}$) was higher than current efficiency (ε_p) at low feed water concentration ($\approx$0.05 mol/l). This was predicted by the following relationship [5]:

$$\eta < \frac{\Delta\psi_m^c + |\Delta\psi_m^a|}{|2\Delta\psi_i|} \tag{56}$$

The above equation is valid if the influence of volume flow is negligible.

The apparent transport number ($\overline{\Delta t}$) decreased with increasing feed concentration. Current efficiency, however, increased with increasing feed water concentration as a result of increasing water flow. Consequently, current efficiency became higher than the apparent transport number at higher (0.5 to 1 mol/l) feed water concentrations. Current efficiency, however, can decrease at very high feed concentrations as a result of back diffusion.

5. Conclusions

(1) Brine concentration increased with increasing current density and feed water concentration. Brine concentration appeared to attain a constant value at high current density dependant upon the electro-osmotic coefficients of the membranes.

(2) Current efficiencies were nearly constant in a wide range of current densities (0 to 70 mA/cm^2) and feed water concentrations (0.05 to 1.0 mol/l). This showed that the limiting current density was not exceeded.

(3) Water flow through the membranes increased with increasing current density and feed water concentration. This increasing water flow improved current efficiency and water flow can therefore also have a positive effect on ED.

(4) The electro-osmotic coefficients were determined to be a function of feed water concentration. The coefficients decreased with increasing feed water concentration until a constant value was obtained at high current density. The decrease in electro-osmotic coefficients with an increase in feed water concentration can be ascribed to deswelling of the membranes with increasing feed water concentration or to a reduction in membrane permselectivity when the feed water concentration is increased.

(5) Osmotic flow in EOP decreases relative to the total flow with increasing current density while the electro-osmotic flow increases relative to the osmotic flow. Osmotic flow, however, contributes significantly to the total water flow in EOP.

(6) Selemion AMV and CMV membranes performed satisfactorily for concentration of sodium chloride solutions. Salt brine concentrations of 19.3% (193 g/l); 25.1% (251 g/l); 27.2% (272 g/l) and 29.8% (298 g/l) were obtained at feed water concentrations of 0.05 (2.925); 0.1 (5.85); 0.5 (29.25) and 1.0 mol/l (58.5 g/l), respectively. Current efficiency in this feed water concentration range varied from 62 to 91%.

(7) It has been demonstrated that a simple potential measurement can be used to predict membrane performance for salt concentration with ED. The ratio between the apparent transport number ($\overline{\Delta t}$) of a membrane pair and current efficiency (ε_p), however, depends on the feed concentration and current density used. Ratios of $\overline{\Delta t}/\varepsilon_p$ varied between 1.0 and 1.13 (0.1 mol/l feed). However, poorer correlations were obtained at lower (0.05 mol/l) and higher (0.5 and 1.0 mol/l) feed concentrations. Consequently, it appears that it should be possible to predict current efficiency for concentration of sodium chloride solutions with an accuracy of ≈10% from the transport number of the membrane pair (at 0.1 mol/l feed).

(8) The correct Onsager relationships to be used for potential measurement ($\Delta\psi$) and for the transport number (*JF/I*) are at zero current and zero volume flow, and at zero concentration gradient and zero volume flow, respectively. In practical, ED measurements are conducted at zero pressure and in the presence of concentration gradients and volume flows. These factors will influence the results considerably in all systems in which volume flow is important and where the concentration factor is high as encountered in EOP. In measurement of membrane potential, the volume flow is against the concentration potential and in general will decrease potential. In ED, water flow helps to increase current efficiency, but the concentration gradient is against the current efficiency.

(9) Brine concentration can be predicted from apparent transport numbers ($\overline{\Delta t}$'s) and water flows through the membranes. The ratio $c_{b\,calc}/c_{b\,exp}$ decreased with increasing feed concentration.

(10) Maximum brine concentration, c_b^{max}, can be predicted from two simple models. A very good correlation was obtained by two methods. Maximum brine concentration increased with increasing feed concentration and appeared to level off at high feed concentration (0.5 to 1.0 mol/l).

6. List of symbols

a_i	activity of species i (mol/l)
A_m	effective membrane area (cm_2)
β_i	drag coefficient associated with the ionic species i
β	electro-osmotic coefficient ($cm^3\ C^{-1}$)
β°	electro-osmotic coefficient measured at low ionic strength
c_i	concentration of species i (mol/l)
c_s	salt concentration (mol/cm^3)
c_b, c_f, c_p	concentration to brine, feed and product, respectively (mol/cm^3)
ε	overall current efficiency
ε_p	Coulomb efficiency (current efficiency)
ε_w	efficiency associated with water transport through membranes
F	Faraday's constant – 96 500 (A s/mol)
g	osmotic coefficient
I	electric current density (A/cm^2)
I_{eff}	effective current density (A/cm^2)
j_i	flux of species i through a membrane ($mol/(s\ cm^2)$)
J	volume flow through a membrane ($cm/s \equiv cm^3/cm^2\ s$)
J_{osm}	osmotic flow
J_{elosm}	electro-osmotic flow
J_v	volume flux ($cm\ s^{-1}$)
L_p	hydraulic permeability $cm\ s^{-1}$ per unit pressure

Q	amount of feed solution entering a dilute channel per unit time ($cm^3\ s^{-1}$)
R	universal gas constant
T	absolute temperature (K)
Δt	difference between counter-ion and co-ion effective transport members
$\overline{\Delta t}$	effective transport number of a membrane pair
$\bar{t}_i$	effective transport number of the ionic species i
μ_i	chemical potential of ionic species i
μ_w	chemical potential of water
V	volume of solution that enters a membrane bag per unit area (ml/cm^2)
x	length coordinate perpendicular to the membrane
z_i	charge of ionic species i (in units of the proton charge)
Λ	degree of demineralization
$\Delta\psi'_m$	electrical potential difference between reversible electrodes, due to a difference of concentration at both sides of the membrane
$\Delta\psi_i$	theoretical potential
σ	reflection coefficient
η	efficiency, current efficiency
π	osmotic pressure

Superscripts

a, c	refers to anion- and cation-exchange membrane
$'$, $''$	refers to feed and effluent solutions

Subscripts

1	counter-ion
2	co-ion
i	identifies ith ion
m	refers to membrane phase
s	salt
w	water

Acknowledgements

The authors wish to express their thanks to the South African Water Research Commission for financial aid. The author also wishes to thank Professor Ora Kedem of the Weizmann Institute of Science in Israel for valuable advice given during execution of the project.

Appendix A

Typical EOP experimental conditions and results are shown in Tables 9–12.

Table 9
Electro-osmotic pumping experimental conditions and results for 0.05 mol/l sodium chloride (Selemion AMV and CMV)

Current density	Brine concentration, c_b (mol/l)		Water flow	Current efficiency	Effective current density	Transport numbers				
I (mA/cm^2)	$c_{b\,exp}$	$c_{b\,calc}$	J (cm/h)	ε_p (%)	I_{eff} (mA/cm^2)	Δt^c	Δt^a	$\overline{\Delta t}$	t_i^c	t_i^a
5	1.62	1.59	0.102	62.37	3.12	0.91	0.82	0.87	0.96	0.91
10	2.15	2.76	0.115	66.22	6.62	0.88	0.82	0.85	0.94	0.91
15	2.65	3.35	0.137	64.79	9.72	0.85	0.78	0.82	0.93	0.89
20	2.81	3.54	0.170	64.93	12.99	0.86	0.75	0.81	0.93	0.88
30	3.31	4.05	0.217	64.15	19.25	0.84	0.73	0.79	0.92	0.86

Electro-osmotic coefficient (2β)=0.219 l/F (slope=0.008194 ml/mAh, Fig. 15).
J_{osm}=y-intercept=0.06023 cm/h (Fig. 15).
$c_b^{max} = 4.55$ mol/l.
$\Delta t^c = t_1^c - t_2^c$.
$2\beta = \frac{0.008194\,ml}{mA/h} \cdot \frac{1000\,mA}{1\,A} \cdot \frac{1\,h}{3600\,s} \cdot \frac{96500\,A\,s}{1\,F} \cdot \frac{1\,l}{1000\,ml} = 0.219\,l/F$.
$c_{b\,cal} = \frac{30\,mA/cm^2 \times 0.79}{(96500\,A\,s/mol)(0.000060265\,ml/cm^2\,s)}(0.217\,cm/h = 1.638\,ml/h) = 4.05\,mol/l$ (Eq. 16).
$\Delta t^a = t_2^a - t_1^a$.
$\overline{\Delta t}$= Average transport number of the membrane pair.
$\bar{t}_1^c$=Transport number of cation through cation membrane.
$\bar{t}_2^a$=Transport number of cation through cation membrane.

Table 10
Electro-osmotic pumping experimental conditions and results for 0.1 mol/l sodium chloride (Selemion AMV and CMV)

Current density	Brine concentration, c_b (mol/l)		Water flow	Current efficiency	Effective current density	Transport numbers				
I (mA/cm^2)	$c_{b\,exp}$	$c_{b\,calc}$	J (cm/h)	ε_p (%)	I_{eff} (mA/cm^2)	Δt^c	Δt^a	$\overline{\Delta t}$	t_i^c	t_i^a
5	1.79	2.1	0.076	73.0	3.65	0.94	0.81	0.87	0.97	0.90
10	2.37	2.64	0.118	74.4	7.47	0.89	0.78	0.84	0.94	0.89
15	2.83	3.02	0.152	76.7	11.51	0.89	0.75	0.82	0.94	0.88
20	3.02	3.21	0.188	76.1	15.23	0.88	0.73	0.81	0.94	0.87
30	3.58	3.74	0.238	76.2	22.86	0.85	0.74	0.80	0.93	0.87
40	3.91	4.09	0.286	75.0	30.01	0.89	0.68	0.78	0.94	0.84
50	4.29	4.33	0.330	75.9	37.95	0.82	0.71	0.77	0.91	0.85

Electro-osmotic coefficient (2β)=0.198 l/F (slope=0.00739 ml/mA h, Fig. 15).
J_{osm}=y-intercept=0.067696 cm/h.
c_b^{max}=5.05 mol/l.
$\Delta t^c = t_1^c - t_2^c$.
$\Delta t^a = t_2^a - t_1^a$.
$\overline{\Delta t}$=Average transport number of membrane pair.
$\overline{t_1^c}$=Transport number of cation through cation membrane.
$\overline{t_2^a}$=Transport number of anion through anion membrane.

Table 11
Electro-osmotic pumping experimental conditions and results for 0.5 mol/l sodium chloride (Selemion AMV and CMV)

Current density	Brine concentration, c_b (mol/l)		Water flow	Current efficiency	Effective current density	Transport numbers				
I (mA/cm^2)	$c_{b\,exp}$	$c_{b\,calc}$	J (cm/h)	ε_p (%)	I_{eff} (mA/cm^2)	Δt^c	Δt^a	$\overline{\Delta t}$	t_i^c	t_i^a
5	1.72	1.71	0.0895	82.5	4.13	0.92	0.71	0.82	0.96	0.86
10	2.74	2.33	0.122	89.66	8.96	0.86	0.67	0.76	0.93	0.83
20	3.54	2.82	0.190	91.72	18.34	0.81	0.63	0.72	0.91	0.81
30	3.94	3.27	0.248	87.35	26.21	0.86	0.59	0.72	0.93	0.80
40	4.20	3.26	0.323	90.89	36.36	0.81	0.60	0.71	0.90	0.80
50	4.50	3.51	0.378	91.23	45.62	0.84	0.58	0.71	0.92	0.79
60	4.66	3.62	0.440	91.46	54.88	0.85	0.57	0.71	0.93	0.79

Electro-osmotic coefficient (2β)=0.187 l/F (slope=0.006959 ml/mA h, Fig. 15).
J_{osm}=y-intercept=0.062409 cm/h.
c_b^{max}=5.36 mol/l.
$\Delta t^c = t_1^c - t_2^c$.
$\Delta t^a = t_2^a - t_1^a$.
$\overline{\Delta t}$=Average transport number of membrane pair.
$\overline{t_1^c}$=Transport number of cation through cation membrane.
$\overline{t_2^a}$=Transport number of anion through anion membrane.

Table 12
Electro-osmotic pumping experimental conditions and results for 1.0 mol/l sodium chloride (Selemion AMV and CMV)

Current density	Brine concentration, c_b (mol/l)		Water flow	Current efficiency	Effective current density	Transport numbers				
I (mA/cm^2)	$c_{b\,exp}$	$c_{b\,calc}$	J (cm/h)	ε_p (%)	I_{eff} (mA/cm^2)	Δt^c	Δt^a	$\overline{\Delta t}$	t_i^c	t_i^a
10	2.95	2.41	0.113	89.00	8.90	0.84	0.62	0.73	0.92	0.81
20	3.73	2.90	0.174	87.14	17.43	0.82	0.55	0.68	0.91	0.77
30	4.12	3.16	0.236	86.95	26.09	0.79	0.55	0.67	0.90	0.78
40	4.55	3.51	0.279	85.21	34.08	0.80	0.51	0.66	0.90	0.76

Table 12
(Continued)

Current density	Brine concentration, c_b (mol/l)		Water flow	Current efficiency	Effective current density	Transport numbers				
I (mA/cm^2)	$c_{b\,exp}$	$c_{b\,calc}$	J (cm/h)	ε_p (%)	I_{eff} (mA/cm^2)	Δt^c	Δt^a	$\overline{\Delta t}$	t_i^c	t_i^a
50	5.07	3.70	0.328	89.28	44.64	0.79	0.52	0.65	0.89	0.76
60	5.10	3.79	0.384	87.52	52.51	0.80	0.50	0.65	0.90	0.75

Electro-osmotic coefficient (2β) = 0.154 l/F (slope=0.005757 ml/mA h, Fig. 15).
J_{osm}=y-intercept=0.078991 cm/h.
c_b^{max}=6.48 mol/l.
$\Delta t^c = t_1^c - t_2^c$.
$\Delta t^a = t_2^a - t_1^a$.
$\overline{\Delta t}$=Average transport number of membrane pair.
$\bar{t}_1^c$=Transport number of cation through cation membrane.
$\bar{t}_2^a$=Transport number of anion through anion membrane.

References

[1] G. Garza, Electrodialysis by electro-osmotic pumping and ion separation with charged membranes. Thesis submitted to the Weizmann Institute of Science, Rehovot, Israel, 1973.

[2] G. Garza and O. Kedem, Electro-osmotic pumping in unit cells, 5th International symposium on fresh water from the sea, 13 (1976) 79–87.

[3] O. Kedem, G. Tanny and G. Maoz, A simple electrodialysis stack, Desalination, 24 (1978) 313–319.

[4] O. Kedem and J. Cohen, EDS-sealed-cell electrodialysis, Desalination, 46 (1983) 291–299.

[5] O. Kedem and Z. Bar-On, Electro-osmotic pumping in a sealed cell ED stack, AIChE symposium series, Industrial Membrane Processes, 248, 81 (1986) 19–27.

[6] J.J. Schoeman, Electrodialysis of salts, acids and bases by electro-osmotic pumping. Thesis submitted to the University of Pretoria, Pretoria, South Africa, 1992.

[7] G. Oren and J. Litan, The state of the solution membrane interface during ion transport across and ion-exchange membrane, J. Physical Chemistry, 78 (1974) 1805.

[8] H.H. Strathman, Electrodialysis, in W.S. Winston Ho and Kamalesk K. Sirkar (Eds.), Membrane Handbook, Van Nostiand Reinhold, New York, 1992.

[9] K.A. Mauritz and A.J. Hopfinger, Structural properties of membrane ionomers. in J.O.M. Bockris, B.E. Conway and R.E. White (Eds.), Modern Aspects of Electrochemistry, Plenum Publishing Corp., Vol. 14, 1982, Chap. 6.

[10] A. Narebska and R. Wodzki, Swelling equilibria and structure variations of nafion and polyethylene (polystyrene sulphonic acid) membranes at high electrolyte cocentrations and increased temperature, Die Angewandte Makromolekulare Chemie, 107 (1982) 51–60 (No. 1679).

[11] C. Rueda, C. Ruiz-Bouza and J. Agular, Electro-osmotic permeability of cellulose acetate membranes, J. Physical Chemistry, 61 (1977) 789.